Science and Global Security, 15:57–83, 2007

ISSN: 0892-9882 print / 1547-7800 online
DOI: 10.1080/08929880701319754

Routledge
Taylor & Francis Group

Impact Deflection of Potentially Hazardous Asteroids Using Current Launch Vehicles

Jesse D. Koenig[1] and Christopher F. Chyba[2]

[1]SpaceDev Inc., Poway, CA, USA
[2]Department of Astrophysical Sciences and Program on Science and Global Security, Woodrow Wilson School of Public and International Affairs, Princeton University, Princeton, NJ, USA

Nuclear explosions, and a wide variety of technologies not yet realized, have been proposed to deflect asteroids away from collision with Earth. In contrast, this article presents realistic models for simple kinetic energy impact deflection, using the actual orbital elements of 795 catalogued Potentially Hazardous Asteroids, and impactor masses launched to intercept trajectories by Atlas V HLV rockets or equivalent. The authors take asteroid diameter, density, cratering characteristics, and Earth-collision lead time as parameters whose influence is to be investigated. Assuming asteroids of rocklike density, the article finds deflection off of Earth-collision to be achievable given 5-year lead time with a single kinetic energy intercept for 100% of 250 m diameter PHAs, 20-year lead with a single intercept for 93% of 500 m PHAs, 20-year lead with 5 and 10 intercepts, respectively, for 55% and 94% of 1 km PHAs, or 100-year lead with 1 and 2 intercepts, respectively, for 55% and 94% of 1 km PHAs. Considering likely future lead times for Near-Earth Objects, simple impact deflection using current launch vehicles is therefore a viable strategy for up to kilometer-diameter asteroids. This method has important advantages over other proposals: it requires no new technologies, would not require development or testing of nuclear warheads, and would likely be the least costly, least risky, and fastest to effect.

Received 19 November 2006; accepted 19 January 2007.
The authors thank K. Holsapple (University of Washington) for discussions of cratering models, and B. Kutter (Lockheed Martin) for the use of Atlas V HLV performance data. This work was partially supported by Carnegie Corporation of New York through the Center for International Security and Cooperation at Stanford University, the MacArthur Foundation, and SpaceDev, Inc.
Address correspondence to Jesse D. Koenig, SpaceDev Inc., 13855 Stowe Drive, Poway, CA 92064, USA. E-mail: jesse@spacedev.com

BACKGROUND

Many techniques for deflecting asteroids away from collision with Earth have been proposed, including nuclear explosions,[1,2] nuclear powered ion propulsion,[3] solar sails,[4] mass drivers,[4] gravity tugs,[5] and more exotic technologies.[6] However, deflection by simple impact,[2,4] were it demonstrated to be viable for large asteroids, would have important advantages over other proposals: it would require no new technologies and would likely be the least costly, least risky, and fastest to effect. It would also be far less politically difficult to develop and test than any option involving nuclear warheads. This article presents realistic models for kinetic energy impact deflection, using the actual orbital elements of 795 catalogued Potentially Hazardous Asteroids (PHAs).[7] The authors take asteroid diameter, density, cratering, and Earth-collision warning (lead) time as parameters whose influence is to be investigated. As the catalogue of the Near-Earth Object (NEO) population orbits expands, lead times for any discovered Earth-colliding objects are likely to be one or two centuries, the time horizon out to which NEO orbits may typically be reliably projected.[8] Simple impact deflection is then a viable strategy even for kilometer-diameter asteroids.

Impacts as large as that of the ~10 km-diameter K/T bolide that struck Earth with $\sim 10^8$ mt of energy occur every ~100 million years.[9] In 1908 an asteroid with diameter ~60 m exploded over Tunguska Siberia, releasing ~10 mt of energy, equivalent to a large nuclear warhead[10]; impacts of this magnitude occur once every ~1,000 years.[11] In between the mass extinction and local destruction impact classes is the global catastrophe class of 1 to 2 km objects, impacting Earth once every ~1 million years.[8]

Efforts to detect, catalogue, and track the NEO population are well under way, with ~85% of the estimated 1,000 NEOs >1 km in diameter discovered by 28 November 2006.[12] The survey is complete for NEOs with diameters >5 km, and for as long as orbits can be reliably predicted (about a century, with subsequent uncertainty due to limits of observation and simulation accuracy, and outcomes of close planetary passes); none of these threatens Earth[8,21]. The characterization of these objects is less mature, and research and development for NEO deflection has barely begun.[13,22]

KINETIC IMPACT DEFLECTION

Kinetic impact deflection entails one or more missions in which a conventional spacecraft launch vehicle delivers a payload of inert mass onto a trajectory to impact the threatening asteroid with a relative impact velocity typically 10–30 km/s. This projectile is attached to a spacecraft bus that provides final precision guidance. The dissipation of the impactor's kinetic energy on impact explosively craters the surface, ejecting asteroid material into space. These

ejecta act as propulsion for the asteroid, imparting momentum in addition to the momentum impulse of the impactor itself.[4]

The impactor is guided to strike a location on the asteroid where the surface is normal to the desired velocity change. This desired ΔV is aligned with, or opposite to, the asteroid's velocity, such that the entire effect goes toward altering the semi-major axis and period of the asteroid's orbit. With every subsequent orbit of the asteroid around the Sun, its position is further diverted from that it would have had without the impact, so the effect accumulates until the asteroid is far enough from its original ephemeris to miss a collision with Earth. A necessary displacement of one Earth radius ($R_\oplus$) is assumed. That is, the asteroid must be deflected such that at the time when the collision with Earth was predicted to occur, the asteroid is displaced by $R_\oplus$ along its orbit from where it otherwise would have been.

In a real scenario, the required displacement distance would depend on the particular orbit of the asteroid and associated uncertainties, relative to Earth's orbit. Most PHAs orbit the Sun in the same sense as Earth, such that if the path of a PHA were to cross Earth's path, the angle between their velocities would be $<90^\circ$, and one would essentially catch up to the other. This geometry, combined with the Earth's spherical shape, cause the required displacement to be less than $R_\oplus$ (not considering orbit uncertainties), even if the asteroid's velocity vector passed directly through the Earth's center at the time of collision. If the vector did not pass through the center, the required displacement would be less still. However, these effects are somewhat offset by gravitational focusing, which makes Earth's effective radius $\sim$1.4 $R_\oplus$ for typical relative velocities.

POTENTIALLY HAZARDOUS ASTEROIDS

Given a 1 $R_\oplus$ displacement requirement, this simulation uses the actual orbital elements of 795 PHAs identified by NASA's NEO Program to determine the technical feasibility of actual rocket payload delivery between Earth and PHA orbits. The NEO Program defines PHAs as those asteroids "with an Earth Minimum Orbit Intersection Distance (MOID) of 0.05 AU or less and an absolute magnitude (H) of 22.0 or less."[7] The *MOID* to Earth indicates the closest possible approach to Earth of the asteroid in its current orbit. Asteroids with a small *MOID* to Earth can become Earth colliders because their orbits change with time due to long-range planetary gravitational perturbations and, particularly, close planetary approaches.[14] $H = 22$ corresponds to a diameter of $\sim$150 m for an albedo of 13% (reference 7), so the majority of PHAs are $>$150 m in diameter. As of 24 July 2005, the PHAs comprised 19% of the Near Earth Objects (Near Earth Asteroids plus Near Earth Comets).[7]

Whereas the orbital elements are well determined for the PHAs, other properties are much less certain. Although there are established visual magnitudes,

the albedo values necessary to convert to size are not well known. Even if the size were known, the density, and therefore mass, would not be. Other generally unknown characteristics are composition, structure, size, and shape. Due to these uncertainties, and because it is instructive to take a parametric approach in the modeling, this analysis uses the orbital elements of the PHAs, but varies other parameters of the hypothetical asteroids together, so that in a given simulation all 795 have the same properties apart from orbital elements.

MODELING THE INTERCEPT TRAJECTORIES

Were a large asteroid predicted to hit Earth, and if kinetic impact were chosen as the deflection method, substantial effort would go into determining an optimal trajectory from the Earth to the asteroid; this would be unique to the particular scenario, and might involve multiply staged thrusting maneuvers and/or gravity assists. However, to model a large number of asteroid missions this analysis uses simpler intercept trajectories calculated via Lambert's method,[15] requiring only one thrusting maneuver (not including the staging that is required to escape Earth's gravity, or small trajectory adjustment maneuvers performed by the spacecraft attached to the impactor). In addition to facilitating a generalized analysis of many asteroids, this approach gives conservative results, as most would be improved by detailed individual analysis of a scenario.

SIMULATION ARCHITECTURE

In each simulation run, 795 hypothetical asteroids are created, with the actual PHA orbital elements and a choice of properties including size, density, and cratering model. Also, a density is selected for the impactor; because higher impactor density gives greater deflection efficiency, the authors typically assume an impactor made of depleted uranium, with density 19 g/cm^3. The authors model the orbital elements a (semi-major axis), e (eccentricity), i (inclination), and ω (argument of perihelion), but do not use actual values for Ω (right ascension of ascending node), or ν (true anomaly). These last two elements would be relevant in describing the orientation of an asteroid's orbit relative to Earth's orbit if Earth's orbit were not considered circular, and in describing the position of each body in its orbit at a specific time. A circular orbit is assumed for Earth, and no *a priori* knowledge of the mission's launch time.

For each hypothetical asteroid, calculate intercept trajectories from various points in the Earth's orbit to various points in the asteroid's orbit, also varying the semi-major axis of the ellipses on which the trajectories lie. Vary the trajectory's semi-major axis from the minimum possible value, a_m, to $2{\cdot}a_m$, in steps of $0.04{\cdot}a_m$. (Overall results improve as the upper limit is raised and as the step size

is decreased, but these are diminishing gains that increase the computational requirements; the upper limit and step size were selected to be a good compromise between maximizing gains and minimizing computation.) Simulation results are stated in terms of a ratio, λ_{mass}, of impactor mass required for adequate deflection to the maximum mass deliverable onto the chosen trajectory by one particular launch vehicle. Rounded up to the next integer, λ_{mass} gives the number of launches required for sufficient deflection to prevent Earth collision.

PROBABILITY OF RESULTS

The most efficient deflection theoretically possible would be found by allowing the impactor to depart any point in Earth orbit and arrive at any point in the asteroid orbit. However, in reality, the resulting ideal Earth-asteroid geometry may never arise. The simulation finds the value of λ_{mass} for which there is a certain probability that this value or lower can be achieved given a certain amount of time to wait for favorable launch geometry of the Earth and asteroid. Using a Monte Carlo analysis, this article reports results for which the probability of achieving those results or better is 60% for 10 years, and 80% for 20 years (Appendix I). That is, for every asteroid, the article reports a value of λ_{mass} (Table 1 and Figure 2) such that at any given point in time, there will be a 60% chance that within the subsequent 10 years, an Earth-asteroid geometry will arise to allow launch into a Lambert intercept trajectory resulting in the reported value or lower. In reality, the trajectory employed may be more sophisticated than the Lambert type used in the present models, allowing it to be more adaptable to current or near term geometry, and thereby reducing the wait-time until launch.

MODELING THE LAUNCH VEHICLE

To assess realistically and conservatively the utility of impact deflection, this article considers only currently available launch vehicles or their equivalent. The two biggest U.S. vehicles are the Boeing Delta IV Heavy Lift Version (HLV), and the Lockheed Martin Atlas V HLV, which have roughly similar capability. The authors chose the Atlas V HLV in the single engine centaur (SEC) upper stage configuration. It is not clear whether the Atlas V HLV will be built, but the comparable Delta IV HLV has already undergone a test flight. NASA is planning to build the Ares V cargo launch vehicle, which will have much greater lift capability than either the Atlas V HLV or Delta IV HLV, but the Ares is not invoked here.

The performance is measured in C3 versus deliverable payload mass. C3 is twice the specific kinetic energy available above Earth escape velocity, that is, a C3 of 0 indicates that the payload can just achieve escape velocity, and a C3 of 100 km^2/s^2 indicates that the payload can be put onto an interplanetary

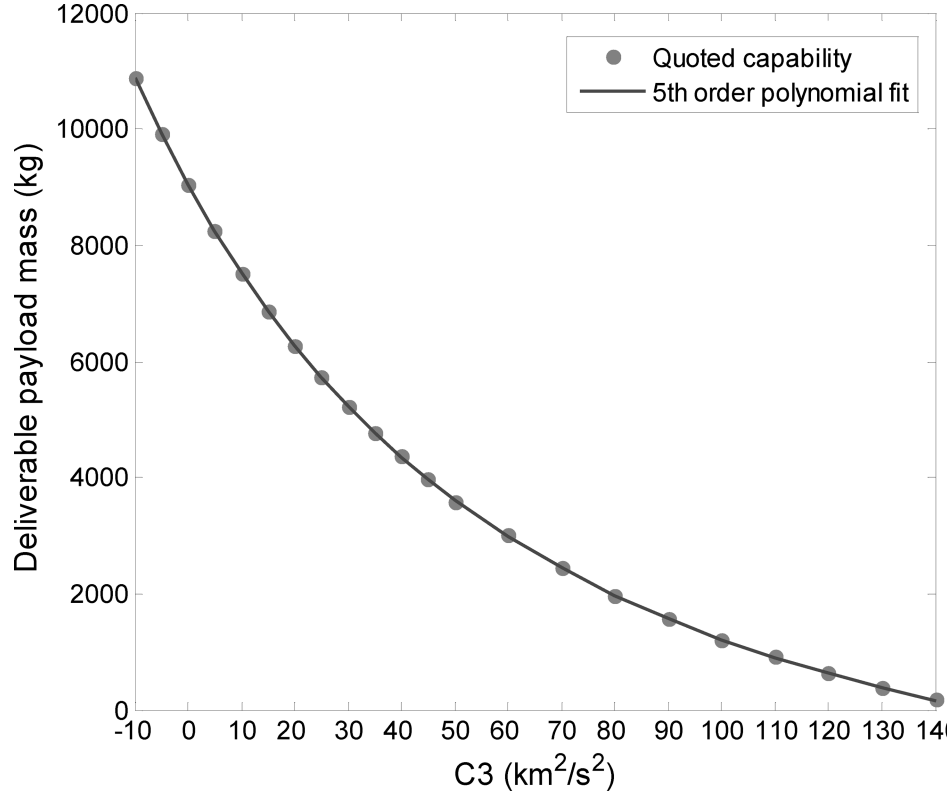

Figure 1: Quoted performance of the launch vehicle,[16] and a 5th order polynomial fit function of this data. The maximum mass fit function is for the launch vehicle payload only. The Atlas V HLV SEC has an option to leave the Centaur upper stage attached to the payload after burnout, which would add another 2,500 kilograms to the asteroid impactor. To be conservative, this is not included in the maximum mass, but is left as a source of margin for the results.

trajectory with a velocity relative to Earth (v_∞) of 10 km/s. For each trajectory analyzed in the simulation, a required C3 is calculated, as well as a required impactor mass. For the required C3, a maximum deliverable mass is calculated using a polynomial fit function of quoted launch vehicle performance values (Figure 1). λ_{mass} is then calculated and used as the metric by which trajectories are selected, and by which overall results are measured.

CALCULATING THE IMPACTOR MASS

To calculate the required impactor mass for a given intercept trajectory, determine the required ΔV to be applied to the asteroid, given by (Appendix II):

$$\Delta V = \frac{2\pi \cdot \delta \cdot a \cdot (1 - e^2)^{0.5}}{3 \cdot t \cdot C \cdot [e \sin\phi \sin\nu + K_\phi (1 + e \cos\nu)]} \tag{1}$$

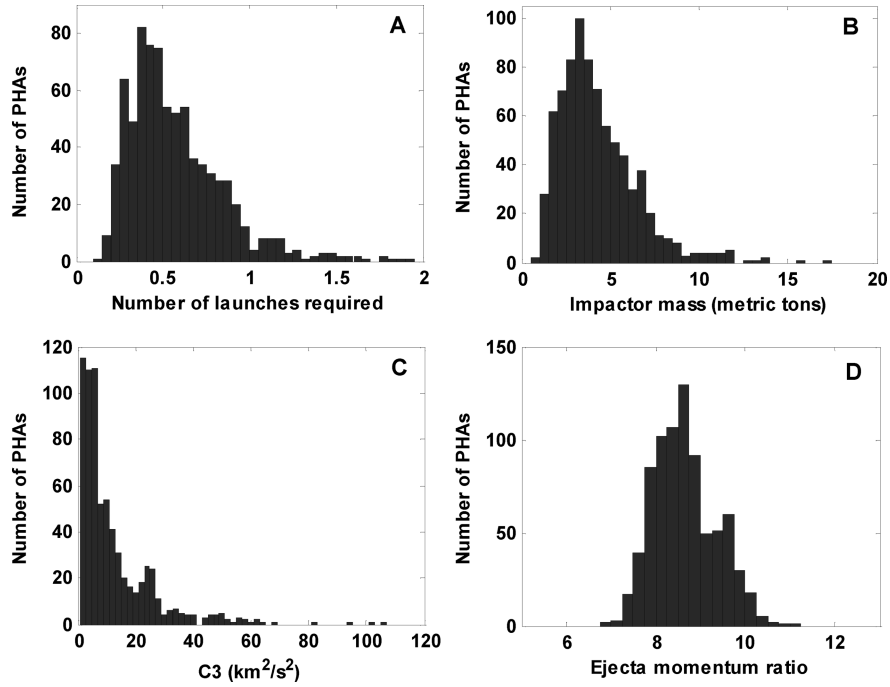

Figure 2: Histograms for simulation 3 (Table 1). In (*A*), "number of launches required" is λ_{mass}.

where ϕ is the flight path angle of the asteroid (the angle between the asteroid's velocity vector and the line normal to the radial vector from the Sun to the asteroid):

$$\phi = \cos^{-1} K_\phi \quad \begin{matrix} \phi(\nu < \pi) > 0 \\ \phi(\nu > \pi) < 0 \end{matrix}, \tag{2}$$

$$K_\phi = \left[\frac{(1 + e\cos\nu)^2}{2(1 + e\cos\nu) - (1 - e^2)} \right]^{0.5}, \tag{3}$$

δ is the required displacement of the asteroid along its orbit at the time of predicted collision with Earth, a is the asteroid orbit semi-major axis, e its eccentricity, ν its true anomaly at the time of perturbation (when it is hit by the impactor), t the time between perturbation and predicted Earth collision, and C the asteroid orbit's circumference (Appendix III).

To find the required impactor mass, use a momentum balance relation (Appendix IV):

$$\Delta V = \frac{m_i V_i |\sin\omega_i|}{m_a} + \frac{\Delta P_{ej}}{m_a - \frac{1}{2} m_{ejT}}, \tag{4}$$

where m_i is impactor mass, V_i the relative impact velocity, ω_i the impact angle, m_a the asteroid mass (asteroids were assumed spherical for mass calculations),

ΔP_{ej} the total ejecta momentum, and m_{ejT} the total ejecta mass. ΔV is found with Equation 1, both V_i and ω_i may be found by analyzing the particular Lambert trajectory, and m_a is essentially a parameter. To solve for m_i one needs a cratering model giving ejecta mass and momentum as a function of known quantities and m_i.

An element of ejecta with mass m imparts a momentum impulse of $m \cdot V_{\text{final}}$, where V_{final} is the velocity of the ejecta relative to the asteroid after it has escaped the asteroid's gravity: $V_{\text{final}} = (V_{ej}^2 - V_{esc}^2)^{0.5}$, where V_{ej} is the initial ejecta velocity relative to the asteroid, and V_{esc} the asteroid's escape velocity at its surface: $V_{esc} = (2G \cdot m_a \cdot r_a^{-1})^{0.5}$, where G is the universal gravitational constant, and r_a the asteroid's radius. A cratering event produces ejecta with a range of initial velocities and therefore a range of V_{final}. ΔP_{ej} is found by integrating over initial velocities:

$$\Delta P_{ej} = \int_{V_{esc}}^{\infty} V_{\text{final}} \cdot \sin\theta \cdot \frac{dm_{ej}}{dV_{ej}} \cdot dV_{ej} \tag{5}$$

where θ is the angle of ejection, taken to be 45° (reference 4), and dm_{ej}/dV_{ej} is derived from an expression[17] for the volume of ejecta Vol_{ej}, with initial velocity $> V_{ej}$:

$$Vol_{ej}(>V_{ej})R^{-3} = K(\sqrt{gR}/V_{ej})^{\zeta}, \tag{6}$$

where R is the radius of the transient (initially excavated) crater, K and ζ are target dependent constants, and g is the asteroid's gravity at its surface. In the cratering literature, ζ is typically denoted as ν; this study uses ζ to avoid ambiguity. A gravity scaling model was chosen to account for an asteroid composed of non-coherent material, or an asteroid of initially coherent material but where the shock of impact fragments the surrounding material—eliminating its inherent strength—ahead of the crater evolution, such that by the time material is excavated, it is no longer coherent.[18]

R may be expressed as a function of g, V_i, m_i, ρ_a (asteroid density), ρ_i (impactor density), and the target dependant constants C_D and β (β is determined by ζ in gravity scaling case; see Appendix V) by combining crater relations (Appendix VI describes the derivation).[19] The impactor mass required to impart a particular ΔV to the asteroid is found to be:

$$m_i = (-B - \sqrt{B^2 - 4AC})/2A \tag{7}$$

where

$$A = k_1 k_4 \tag{8}$$

$$B = -\Delta V \cdot k_3 k_4 - k_1 k_3 - k_2 k_3 \tag{9}$$

$$C = \Delta V \cdot k_3^2 \tag{10}$$

and

$$k_1 = V_i|\sin\omega_i| \tag{11}$$

$$k_2 = \sin\theta \cdot \zeta K C_D^{3+\zeta/2} 2^{\frac{3(1+\beta)}{\beta-1}} V_i^{\zeta} \rho_a^{-\zeta/6} \rho_i^{\zeta/6} \cdot \int_{V_{esc}}^{\infty} \left(V_{ej}^2 - 2\mu_a/r_a\right)^{0.5} V_{ej}^{-\zeta-1} dV_{ej} \tag{12}$$

$$k_3 = m_a \tag{13}$$

$$k_4 = \frac{1}{2} K C_D^{3+\zeta/2} 2^{\frac{3(1+\beta)}{\beta-1}} V_i^{\zeta} \rho_a^{-\zeta/6} \rho_i^{\zeta/6} V_{esc}^{-\zeta} \tag{14}$$

CRATERING MODELS

This study employs a set of cratering constants determined experimentally with dry Ottawa sand as the target material:[17,19] $K = 0.32$, $\zeta = 1.22$, and $C_D = 1.68$. This is the most conservative set, in that it yields the lowest ejecta momentum ratio the authors have found in the literature. The ejecta momentum ratio is the ratio of the total momentum of ejecta to the momentum of the impactor, both relative the asteroid. This is not the ratio of effective momenta as they apply to imparting the desired ΔV. The effective ejecta momentum is the total ejecta momentum multiplied by the sine of the ejection angle, taken to be 45° (reference 4). (By stipulating that the impactor is guided to strike the asteroid on a surface normal to the desired ΔV, it is assumed that the ejecta are aimed in the optimal direction regardless of impact velocity direction.) The effective impactor momentum is the momentum of the impactor multiplied by the sine of the impact angle, which ranges from 0 to 90°, depending on the asteroid orbit and the intercept trajectory.

In the simulations the Ottawa sand model yields an ejecta momentum ratio between 5 and 17 (e.g. Figure 2D). A cratering model due to Holsapple[20] suggests a momentum ratio of 38.5, and the authors have run simulations with this assumption as well. In reference 20, Equation 6.6 should be:

$$P = \int_{V_1}^{V_2} V dM = \frac{1.65(0.06)}{0.65} mU\left(\left(\frac{V_1}{U}\right)^{-0.65} - \left(\frac{V_2}{U}\right)^{-0.65}\right). \tag{15}$$

Dr. Holsapple confirmed this correction on 24 July 2006 via personal communication. Equation 6.7 in reference 20 should then be: $P = 38.5\ mU$, indicating an ejecta momentum ratio of 38.5, instead of 13.6. Finally, to serve as a worst case model and to address concerns over highly porous NEOs that may produce very little ejecta[20], the authors have simulated impacts with no ejecta.

RESULTS

Results are summarized for selected simulations (Table 1), and shown in more detail for a particular simulation (Figure 2).

BINARY ASTEROIDS

It is estimated that ~15% of Near Earth Asteroids larger than 200 m in diameter are binary asteroids.[23] Kinetic energy impact might be somewhat more challenging in its execution for binary asteroids, but in the vast majority of cases would be equally as effective as for single asteroids. When impacting a body in a binary system, there are several possible effects; Case 1: The resulting ΔV to the impacted body is large enough and in the right direction to break the binary orbit, causing divergence of the two bodies; Case 2: The ΔV does not cause divergence of the two bodies, but causes their orbit to go unstable such that the bodies collide and stick together, forming a single body; Case 3: The two bodies remain in orbit around each other.

In Cases 2 and 3, where the two bodies remain bound together, the result of an impact to either body in the binary system would be the same for purposes of deflection as that of an impact to a single asteroid. Momentum is conserved, so the impulse imparted to one of the bodies would be imparted to the entire system, and the resulting ΔV to the system would be the same as for a single asteroid of similar mass. In Case 1, both bodies after divergence may have trajectories sufficiently different than that of the original binary system as to give deflection off of Earth-collision. However, Case 1 also entails more uncertainty, and more risk that one of the bodies would not be adequately deflected.

Case 1 would require the imparted ΔV to be at least as great as the difference between the bodies' relative velocity and their mutual escape velocity. For a binary system with two bodies of total mass m_T and separation distance d in circular orbits about their center of mass (C_m), the relative velocity is $V_{rel} = \sqrt{Gm_T/d}$ and the mutual escape velocity is $V_{eM} = \sqrt{2} \cdot V_{rel}$. For given m_T and d, Case 1 is less likely to occur for systems with greater disparity between the sizes of the two bodies, assuming an impact to the larger body. Therefore, Case 1 is most likely for two bodies of the same size.

Consider a binary asteroid system with two 400 m bodies (roughly the same total mass as a single 500 m asteroid) of density 3 g/cm^3, as represented in Figure 3. At 23 km separation distance, the minimum required ΔV applied to either of the bodies for the system to permanently diverge is 10 mm/s with the ΔV exactly parallel to the impacted body's velocity relative to the C_m. Figure 4 shows that for a 20-year lead time, the required ΔV for deflection is less than 5 mm/s for the vast majority of PHAs. This threshold corresponds to 10 mm/s applied to a body in a binary system of two equal masses. Thus, for the binary asteroid of two 400 m, 3 g/cm^3 bodies separated by 23 km or less, the

Table 1: Summary of selected simulations. For all simulations represented, total deflection distance is one Earth radius, and the probability of achieving these results or better (i.e., these percentages or higher of PHAs that can be deflected with a certain number of launches) is 60% with 10 years to achieve favorable Earth-asteroid geometry, and 80% with 20 years.

Simulation	Asteroid diameter (m)	Asteroid density (g/cm^3)	Impactor density (g/cm^3)	Time from deflection impact to predicted Earth collision (years)	Crater model	Number of launches/ Percentage of PHAs that can be deflected with that number of launches or fewer	
1	1000	3	19	100	Ottawa sand	1/55%	2/94%
2	1000	3	19	20	Ottawa sand	5/55%	10/94%
3	500	3	19	20	Ottawa sand	1/93%	2/100%
4	250	3	19	5	Ottawa sand	1/100%	
5	1000	3	8.9	100	Ottawa sand	1/44%	2/91%
6	1000	1.5	19	100	Ottawa sand	1/97%	2/100%
7	1000	0.5	19	20	Ottawa sand	1/95%	2/100%
8	500	1.5	19	10	Ottawa sand	1/100%	
9	500	0.5	19	3	Ottawa sand	1/99%	2/100%
10	1000	3	NA	50	P ratio = 38.5	1/99%	2/100%
11	1000	3	NA	100	No ejecta	10/57%	30/97%
12	750	0.5	NA	100	No ejecta	1/74%	2/95%
13	400	3	NA	100	No ejecta	1/78%	2/97%
14	500	0.5	NA	20	No ejecta	1/54%	3/96%
15	250	3	NA	20	No ejecta	1/71%	3/99%
16	250	1.5	NA	20	No ejecta	1/92%	2/100%
17	250	0.5	NA	5	No ejecta	1/86%	2/99%
18	150	3	NA	20	No ejecta	1/100%	

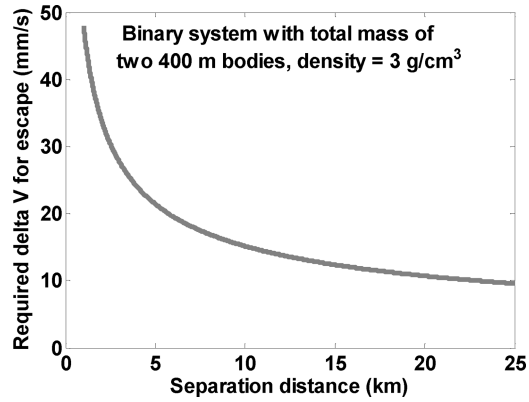

Figure 3: For a binary asteroid system with total mass equal to two 400 m bodies of density 3 g/cm^3, minimum required ΔV applied to either body to achieve mutual escape velocity, as a function of the bodies' separation distance.

required ΔV for deflection with 20-year lead would be less than the minimum required ΔV for divergence, and divergence could not occur with an appropriate deflection impact. Even with lower divergence ΔV or higher deflection ΔV, the impact could be timed such that the ΔV was not parallel to the impacted body's velocity relative to the C_m, the ΔV would not increase the velocity's magnitude, and divergence would not occur.

So, for binary asteroids, impact deflection in Cases 2 and 3 would give effectively the same result as for a single asteroid, while Case 1 is very unlikely to occur. Moreover, adequate deflection may be achieved even in Case 1. Probably the biggest difference in impacting a binary system would be the added challenges in targeting and guiding the impactor.

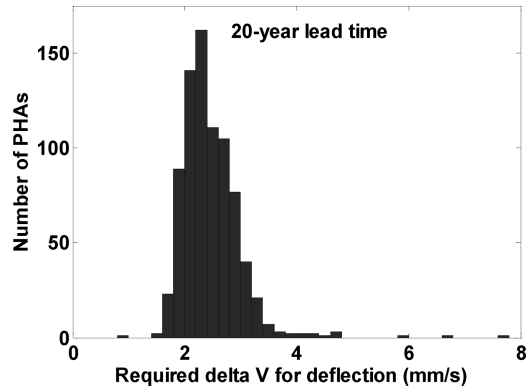

Figure 4: Histogram for the PHAs of required ΔV for a 1 $R_\oplus$ deflection with a 20-year lead time.

CONCLUSIONS

Assuming lead time of two decades, simple impact is an effective deflection method with few launches (1 to 3) for PHAs up to 500 m, either with rocklike density (3 g/cm^3) and significant cratering ejecta, or with low density (0.5 g/cm^3) and no ejecta—encompassing the majority of potential threats. It is important to note that the authors make no assumptions of extraordinary amounts of ejecta. In fact, their cratering model gives ejecta momentum ratios far lower than some others found in the literature (e.g., the ratios shown in Figure 2D, typically in the range 8 to 10, versus the ratio of 38.5 in the model due to Holsapple[20]). Different asteroids have different physical properties, so will have different cratering behavior; porous and incoherent asteroids may give very little ejecta, and therefore the authors also simulated impacts with zero ejecta to provide a worst case extreme in this regard.

Assuming lead time of a century and few launches, impact deflection is effective with significant cratering for the vast majority of rocklike PHAs up to 1 km, and without ejecta for 400 m rocklike PHAs or 750 m low-density PHAs. Furthermore, because of its simplicity, technological readiness, and low risk level, kinetic energy impact may still be the preferred option in the case that more numerous launches are required, for especially large asteroids or short warning times. With 20-year lead, five and ten intercepts will successfully deflect 55% and 94%, respectively, of 1 km rocklike PHAs.

The greatest source of uncertainty for simulating impact deflection is the cratering model, which dictates the momentum imparted by ejecta. Theoretical and experimental cratering study is ongoing and the authors' analysis framework allows other crater models to be incorporated, which may give them tangible implications regarding asteroid deflection. Particularly, scaled-down asteroid deflection space missions (i.e., practice missions) will be very valuable as proof-of-concept, and also in improving the ability to predict asteroids' cratering dynamics, especially as they correlate to remote sensing observations of asteroids. Moreover, as shown by NASA's Deep Impact mission, such investigations are simultaneously likely to yield substantial scientific results related to small body composition and physical structure.

Besides the need for practice missions, the results suggest that an increased investment in remote NEO sensing may greatly increase the potential utility of impact deflection in several ways. Higher fidelity sensing of NEOs allows higher accuracy orbit determination, which in turn gives longer lead times, increasing the efficacy of impact deflection proportionally. Also, an important aspect of a deflection mission—whether practice or real threat avoidance—is measuring the effect of the impact, that is, measuring the imparted ΔV. This measurement may be achieved with a second observer spacecraft, as in Deep Impact and ESA's planned Don Quijote mission, or it may be done with high fidelity ground-based sensing. Especially for practice missions, ΔV measurement from the ground

may eliminate the need for the observer spacecraft, drastically reducing the mission's cost and complexity. Finally, high fidelity ground-based sensing may be used to characterize the target asteroid before a mission, giving insight as to its size, shape, structure, density, spin-rate, and single versus binary nature. All of this knowledge will be helpful in planning a more effective deflection mission, and will also build capability to predict kinetic impact effects for a given NEO based on prior observations of it. For all of these remote sensing applications, interplanetary radar, such as that from the Arecibo facility in Puerto Rico, may be the most effective technology currently available.

Impact is a relatively inexpensive and simple asteroid deflection method that does not require nuclear weapons or exotic technology development, and will be effective in all but the most severe threat scenarios. The method and its advantages can be capitalized on by investing in high-fidelity remote sensing of NEOs such as with radar, and by beginning a series of scaled-down practice space missions.

NOTES AND REFERENCES

1. V. A. Simonenko, V. N. Nogin, D. V. Petrov, O. N. Shubin, and J. C. Solem. "Defending the Earth against Impacts from Large Comets and Asteroids." *Hazards Due to Comets and Asteroids*, T. Gehrels, Ed. (Univ. of Arizona Press, Tucson, 1994): 929–953.

2. T. J. Ahrens, and A. W. Harris. "Deflection and Fragmentation of Near-Earth Asteroids." *Hazards Due to Comets and Asteroids*, T. Gehrels, Ed. (Univ. of Arizona Press, Tucson, 1994): 897–927.

3. R. L. Schweickart, E. T. Lu, P. Hut, and C. R. Chapman. "The Asteroid Tugboat." *Scientific American* (November 2003): 54–61.

4. H. J. Melosh, I. V. Nemchinov, and Y. I. Zetzer, "Non-Nuclear Strategies for Deflecting Comets and Asteroids." *Hazards Due to Comets and Asteroids*, T. Gehrels, Ed. (Univ. of Arizona Press, Tucson, 1994): 1111–1132.

5. E. T. Lu, and S. G. Love. "Gravitational Tractor for Towing Asteroids." *Nature* 438 (2005): 177–178.

6. C. Gritzner, & R. Kahle. "Mitigation Technologies and Their Requirements." *Mitigation of Hazardous Comets and Asteroids*, M. J. S. Belton, T. H. Morgan, N. Samarasinha, and D. K. Yeomans, Eds. (Cambridge Univ. Press, Cambridge, 2004): 167–200.

7. D. Yeomans. *NASA Near Earth Object Program website* (2006; http://neo.jpl.nasa.gov/neo/groups.html).

8. D. Morrison. "Defending the Earth against Asteroids: The Case for a Global Response." *Sci. Global Sec.* 13(1–2) (2005): 87–103.

9. D. Morrison, C. R. Chapman, and P. Slovic. "The Impact Hazard." *Hazards Due to Comets and Asteroids*, T. Gehrels, Ed. (Univ. of Arizona Press, Tucson, 1994): 59–91.

10. C. F. Chyba, P. J. Thomas, and K. J. Zahnle. "The 1908 Tunguska Explosion: Atmospheric Disruption of a Stony Asteroid." *Nature* 361 (1993): 40–44.

11. M. Di Martino, and A. Cellino. "Physical Properties of Comets and Asteroids Inferred from Fireball Observations."*Mitigation of Hazardous Comets and Asteroids*, M.

J. S. Belton, T. H. Morgan, N. Samarasinha, and D. K. Yeomans, Eds. (Cambridge Univ. Press, Cambridge, 2004): 153–166.

12. D. Yeomans. *NASA NEO Program website, Frequently Asked Questions* (2006; http://neo.jpl.nasa.gov/faq).

13. M. J. S. Belton. "Towards a National Program to Remove the Threat of Hazardous NEOs." *Mitigation of Hazardous Comets and Asteroids*, M. J. S. Belton, T. H. Morgan, N. Samarasinha, and D. K. Yeomans, Eds. (Cambridge Univ. Press, Cambridge, 2004): 391–410.

14. T. Bowell, & B. Koehn. *Minimum Orbital Intersection Distance* (1996, Lowell Observatory; http://www.lowell.edu/users/elgb/moid.html).

15. J. A. Prussing, and B. A. Conway. "Lambert's Problem." *Orbital Mechanics* (Oxford Univ. Press, Oxford, 1993): 62–79.

16. Atlas V performance chart obtained October 28, 2003 via personal communication from Bernard Kutter, Manager of Advanced Launch Systems, Lockheed Martin; used with permission.

17. K. R. Housen, R. M. Schmidt, and K. A. Holsapple. "Crater Ejecta Scaling Laws: Fundamental Forms based on Dimensional Analysis."*J. of Geophysical Research* 88(B3) (1983): 2485–2499.

18. E. Asphaug, and H. J. Melosh. "The Stickney Impact of Phobos: A Dynamical Model." *Icarus* 101 (1993): 144–164.

19. K. A. Holsapple, and R. M. Schmidt. "On the Scaling of Crater Dimensions." *J. of Geophysical Research* 87(B3) (1982): 1849–1870.

20. K. A. Holsapple. "About Deflecting Asteroids and Comets." *Mitigation of Hazardous Comets and Asteroids*, Belton, M. J. S., Morgan, T. H., Samarasinha, N. and Yeomans, D.K., Eds. (Cambridge Univ. Press, Cambridge, 2004): 113–140.

21. C. Gritzner, K. Dürfeld, J. Kasper, and S. Fasoulas. "The Asteroid and Comet Impact Hazard: Risk Assessment and Mitigation Options." *Naturwissenschaften* 93 (2006): 361–373.

22. A. Carusi, G. B. Valsecchi, G. D'Abramo, and A. Boattini. "Deflecting NEOs in Route of Collision with the Earth." *Icarus* 159 (2002): 417–422.

23. J. L. Margot, et. al. "Binary Asteroids in the Near-Earth Object Population." *Science* 296 (2002): 1445–1448.

APPENDICES

Appendix I: Description of Trajectory Selection and Associated Probabilities

Consider an analysis in which there is a fixed circular Earth orbit, and a fixed asteroid orbit given by the orbital elements a, e, i, and ω. Intercept trajectories will go from a test point somewhere on the Earth's orbit to 12 fixed test points on the asteroid's orbit: 10 equally spaced at 36° apart and starting at 0°, and one on each of the ecliptic nodes (the points where the asteroid orbit crosses the plane of Earth's orbit). The nodes are included because they allow trajectories that remain in the ecliptic plane, and these are often optimal because they

do not require energy-intensive out-of-plane thrusting. Also, included in the 10 equally spaced points is perihelion, which is generally the most efficient point in an orbit to apply ΔV for the purpose of changing a. However, in any given deflection scenario, it may not be the optimal impact point, due to considerations of C3 and impact velocity for each trajectory.

Now, Lambert's method is used to calculate a number of different trajectories from the Earth test point to the asteroid test point. A required C3 is calculated for each trajectory. The trajectories with C3 values <140 km^2/s^2 (highest value for which Atlas V HLV SEC performance is quoted) are analyzed further.

For a given point in a particular asteroid orbit, a given lead time before the hypothetical predicted Earth collision, and a given required asteroid displacement at the time of predicted Earth collision, a required asteroid ΔV to be applied to the asteroid is calculated. Knowing the required ΔV, the asteroid's orbit, the intercept trajectory, the asteroid's properties, and the cratering dynamics, calculate the required impactor mass to effect the required ΔV. Also, using the polynomial fit function for launch vehicle performance, calculate the maximum mass that can be launched with the specified C3. Then calculate λ_{mass}, and select the trajectory with the lowest (best) value, to be called λ_{massMin}.

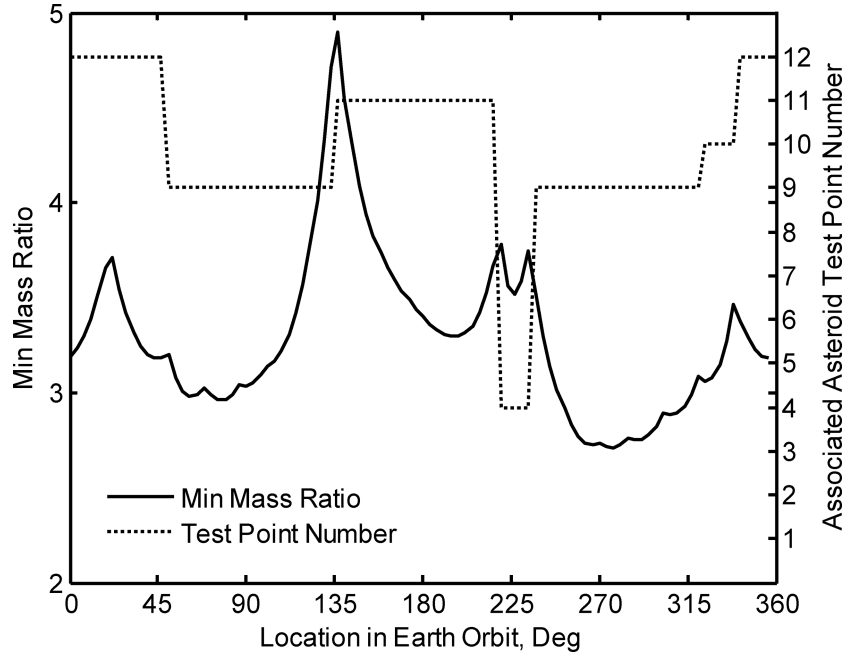

Figure A1: The Minimum Mass Ratio (λ_{massMin}) function for one of the hypothetical asteroids, and the associated asteroid test point (*ast_point*$_{\text{min}}$) numbers. Each interval over which *ast_point*$_{\text{min}}$ is constant is called a region.

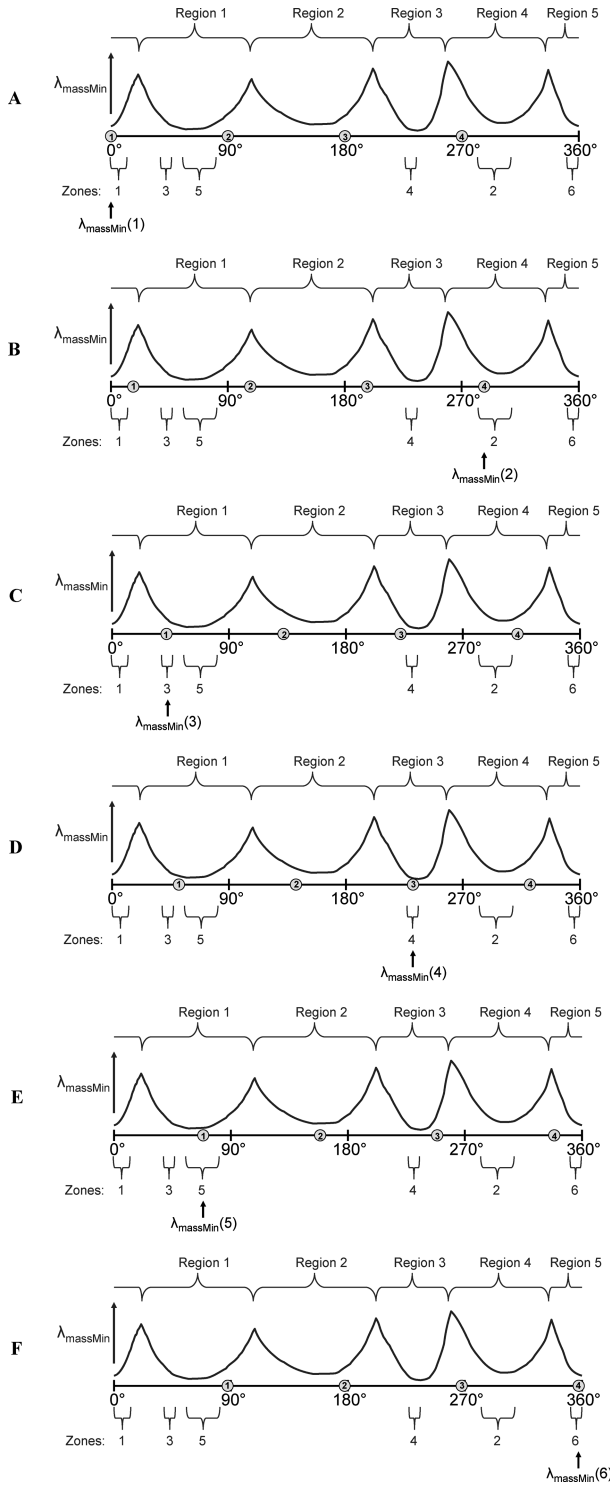
A
B
C
D
E
F
Region 1
Region 2
Region 3
Region 4
Region 5
λmassMin
0°
90°
180°
270°
360°
Zones: 1 3 5 4 2 6
λmassMin(1)
λmassMin(2)
λmassMin(3)
λmassMin(4)
λmassMin(5)
λmassMin(6)

Imagine that this is done with the Earth test point at all different positions in the Earth orbit, and always with the same 12 asteroid test points. Then get a function of $\lambda_{\mathrm{massMin}}$ versus Earth orbit position. Now, define "regions" of the $\lambda_{\mathrm{massMin}}$ function to be the angular intervals in the Earth orbit over which the associated asteroid test point (call this ast_point_{min}) is constant. For the case shown in Figure A1, there are six regions.

In the simulation, do the analysis as described so far, except have four Earth test points, equally spaced at 90° apart. When calculating trajectories and λ_{mass} values, go from each of the four Earth test points to each of the 12 asteroid test points and pick the one trajectory with $\lambda_{\mathrm{massMin}}$ from all of these. Then, incrementally step all four Earth orbit test points (by 1°) together around the Earth orbit relative to the asteroid orbit, leaving the asteroid orbit test points fixed. At each incremental step, find the trajectory with $\lambda_{\mathrm{massMin}}$. Increment the Earth test points through a shift range (90°) equal to the spacing between the Earth test points. This way, all locations (at 1° steps) on the Earth orbit are tested by one of the Earth orbit test points.

As the Earth test points are incremented through the shift range, the one associated with the $\lambda_{\mathrm{massMin}}$ trajectory (call this $Earth\_point_{\mathrm{min}}$) will be in one region of the $\lambda_{\mathrm{massMin}}$ function (Figure A1) for some number of increments, and then will be in another region, that is, ast_point_{min} will change. This transition could coincide with $Earth\_point_{\mathrm{min}}$ switching to a different one of the four Earth test points, or remaining on the same Earth test point. The range of increments over which $Earth\_point_{\mathrm{min}}$ is in one region (i.e., has a constant ast_point_{min}) is called a "zone." The lengths of all the zones add up to the length of the shift range, which is the same as the Earth point spacing, 90° (Figure A2).

From all the $\lambda_{\mathrm{massMin}}$ values obtained throughout the shift range, the worst (highest) one—call this $\lambda_{\mathrm{massMinW}}$—is recorded, representing the worst case that can be expected as long as the Earth is ever in one of the zones while the asteroid is located such that it will be at the test point corresponding to that zone, in

←

Figure A2: Regions and zones illustrated with six steps in the process of incrementing the Earth test points. (For simplicity of the diagram, the regions are shown here as bounded by local maxima in the $\lambda_{\mathrm{massMin}}$ function, but this is not always the case, as shown in Figure A1.) In the present simulations, the Earth test points are stepped in 1° increments through the 90° shift range. Here are 6 of those 90 steps: **(A)** The Earth test points are at 0°, 90°, 180°, and 270°. Earth test point 1 has the lowest value of $\lambda_{\mathrm{massMin}}$, and so the overall $\lambda_{\mathrm{massMin}}$ for this first step, $\lambda_{\mathrm{massMin}}(1)$, is there, in Region 5. Also, it is in the first zone of the incrementing process, which is called Zone 1. **(B)** The Earth test points have been shifted forward. Now Earth test point 4 has the lowest value of $\lambda_{\mathrm{massMin}}$, and so for this second illustrated step,$\lambda_{\mathrm{massMin}}(2)$ is there, in Region 4. Because the region associated with the overall $\lambda_{\mathrm{massMin}}$ has changed, the zone has also changed, from Zone 1 to Zone 2. **(C)** The Earth test points have been shifted further forward, and $\lambda_{\mathrm{massMin}}(3)$ is associated with Earth test point 1, Region 1, and Zone 3. **(D)** $\lambda_{\mathrm{massMin}}(4)$ is associated with Earth test point 3, Region 3, and Zone 4. **(E)** $\lambda_{\mathrm{massMin}}(5)$ is associated with Earth test point 1, Region 1, and Zone 5. **(F)** $\lambda_{\mathrm{massMin}}(6)$ is associated with Earth test point 4, Region 5, and Zone 6.

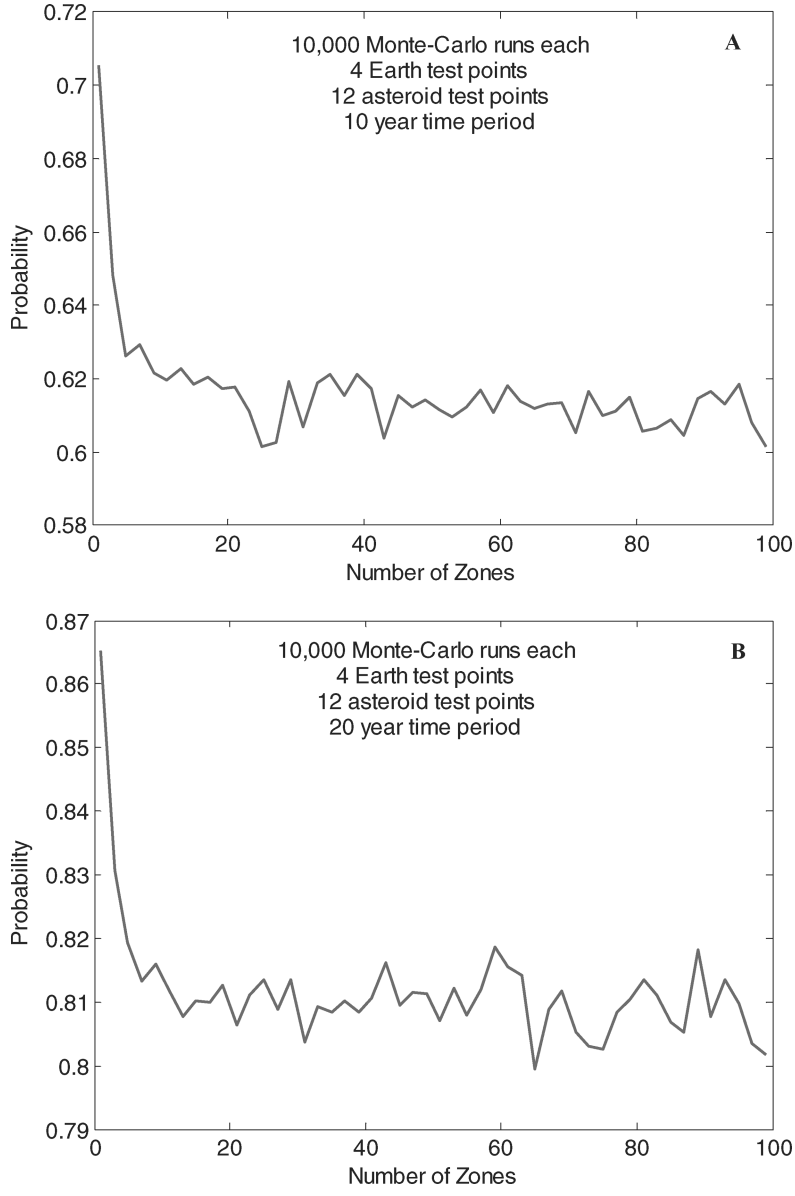

Figure A3: Probabilities of achieving an Earth-asteroid geometry that gives $\lambda_{massMinW}$ or better, over **(A)** a 10-year period, and **(B)** a 20-year period. It is unknown how many zones will exist for a particular asteroid, but one needs to input a number of zones to the Monte-Carlo analysis. Here calculate the probabilities for different numbers of zones from 1 to 99, with 4 Earth test points, 12 asteroid test points, and 10,000 Monte-Carlo runs for each probability calculation. In both (*A*) and (*B*), as the number of zones increases, the probability initially decreases significantly, but then levels off and fluctuates due to its random components. It settles around 81% for the 20-year case, and 61% for the 10-year case.

the amount of time required to traverse the corresponding intercept trajectory. (In Figure A2, $\lambda_{\text{massMinW}} = \lambda_{\text{massMin}}(2)$.)

A separate Monte-Carlo simulation calculates the probability that this situation will arise in some given amount of time. Each run of this simulation includes Earth in its orbit, and a hypothetical asteroid with an orbit selected randomly from among the limits of real PHA orbital elements. A certain number of zones are defined, with random locations, angular widths randomly apportioned from a total equal to the shift range—in this case, 90°, and one of the fixed asteroid test points randomly assigned to each. Both Earth and the asteroid are initialized to random locations in their respective orbits. Then the simulation examines every moment in time when the asteroid is at one of its test points, and calculates whether the Earth was in the corresponding zone at the corresponding time. If the answer is "yes" at least once in the allowed time period, the condition has been satisfied. The percentage resulting from the Monte-Carlo analysis is the number of runs where the condition was satisfied divided by the total number of runs.

A longer allowed time period increases the probability that the condition can be met, although not proportionally. Also, the probability increases as the sum of the angular lengths of the zones increases. This corresponds to a lower number of Earth test points and an inversely greater Earth test point spacing and shift range. However, this would also result in a worse (higher) value of $\lambda_{\text{massMinW}}$. The Monte-Carlo analysis gives the probability that the lowest achievable value of λ_{mass} for a particular asteroid over an allowed time range will equal $\lambda_{\text{massMinW}}$ or better (lower).

To be conservative, round down slightly from the results shown in Figure A3, and say that the probability of achieving the stated results is 60% if there are 10 years to achieve favorable launch geometry among the Earth and asteroid, and 80% if there are 20 years. Again, in reality, the trajectory employed may be more sophisticated than the Lambert type used in the present models, allowing it to be more adaptable to any current or near term geometry, such that the wait time until launch would likely be less than 10 years.

Appendix II: Derivation of Required ΔV

Assuming a change in velocity, ΔV, applied in the direction of, or opposite to the asteroid's velocity, find the ΔV necessary to deflect along its orbit by some distance, δ in some time, t.

Start with the perturbation equation for the semi-major axis in a Keplerian orbit due to a perturbing force:[1,2]

$$\frac{da}{dt} = 2a^{1.5}[\mu(1-e^2)]^{-0.5}[R \cdot e \sin \nu + T(1 + e \cos \nu)] \qquad \text{(A2.1)}$$

where a is the asteroid orbit semi-major axis, μ is the Sun's gravitational constant, e is the asteroid orbit eccentricity, ν is the asteroid's true anomaly when

the perturbation is applied, R is acceleration (force per unit mass) applied along the radial direction (from the Sun to the asteroid), and T is the transverse acceleration applied normal to the radial direction, positive in the direction of the asteroid's velocity.

Define F to be the total acceleration applied, then:

$$R = F\sin\phi \quad \text{and} \quad T = F\cos\phi \tag{A2.2}$$

where ϕ is the flight path angle of the asteroid:

$$\phi = \cos^{-1} K_\phi \quad \begin{matrix} \phi(\nu < \pi) > 0 \\ \phi(\nu > \pi) < 0 \end{matrix} \tag{A2.3}$$

and

$$K_\phi = \left[\frac{(1+e\cos\nu)^2}{2(1+e\cos\nu)-(1-e^2)}\right]^{0.5}. \tag{A2.4}$$

$$\text{Now: } da = 2a^{1.5}[\mu(1-e^2)]^{-0.5}[\sin\phi\cdot e\sin\nu + K_\phi(1+e\cos\nu)]\cdot F\cdot dt \tag{A2.5}$$

$$\text{and the asteroid orbit period is } P = 2\pi\cdot a^{1.5}\mu^{-0.5}. \tag{A2.6}$$

$$\text{So: } \Delta a = \frac{P}{\pi}(1-e^2)^{-0.5}[e\sin\phi\sin\nu + K_\phi(1+e\cos\nu)]\cdot\Delta V, \tag{A2.7}$$

where $F{\cdot}dt$ integrated over the time of impact is just the momentum impulse per unit mass, or ΔV. One orbit after the perturbation, the deflection is:

$$\delta_1 = \frac{\Delta P}{P}C \tag{A2.8}$$

where C is the circumference of the asteroid orbit and is approximated by a formula due to Ramanujan:[3]

$$C \approx \pi(a+b)\left[1+\frac{3x^2}{10+\sqrt{4-3x^2}}\right]$$

$$x = \frac{a-b}{a+b} \tag{A2.9}$$

where b is the asteroid orbit semi-minor axis. Since

$$\frac{dP}{da} = 3\pi\left(\frac{a}{\mu}\right)^{0.5}, \quad \text{one can write} \tag{A2.10}$$

$$\frac{\Delta P}{P} = 1.5\frac{\Delta a}{a}. \tag{A2.11}$$

Over multiple orbits (of number N), the total deflection, δ, will be:

$$\delta = \delta_1 N \quad \text{with } N = \frac{t}{P} \tag{A2.12}$$

So:

$$\delta = \frac{1.5P}{\pi \cdot a}(1 - e^2)^{-0.5}[e \sin\phi \sin + K_\phi(1 + e\cos v)] \cdot C \cdot N \cdot \Delta V \tag{A2.13}$$

Finally:

$$\Delta V = \frac{2\pi \cdot \delta \cdot a \cdot (1 - e^2)^{0.5}}{3 \cdot t \cdot C[e \sin\phi \sin v + K_\phi(1 + e\cos v)]} \tag{A2.14}$$

APPENDIX III: DERIVATION OF FLIGHT PATH ANGLE, ϕ

The flight path angle, ϕ, of an object in orbit about a central body (e.g., an asteroid about the Sun) is the angle between the object's velocity vector, **v**, and the line normal to the radial vector, r, from the central body to the object, as illustrated in Figure A4. ϕ is defined to be positive in the first half of the orbit (true anomaly between 0 and π), and negative in the second half of the orbit. Here derive an expression for ϕ as a function of the object's position in orbit (given by the true anomaly, ν), and the orbit's eccentricity, e.

Equations A3.1–A3.3, A3.5, and A3.6 can be found in reference 4.

The radial distance, r, is given by:

$$r = \frac{p}{1 + e\cos\nu} \tag{A3.1}$$

where the parameter, p, is defined by:

$$p = \frac{h^2}{\mu} \tag{A3.2}$$

where μ is the central body's gravitational constant, and h is the object's specific angular momentum, given by:

$$h = rV\cos\phi \tag{A3.3}$$

where V is the object's velocity.

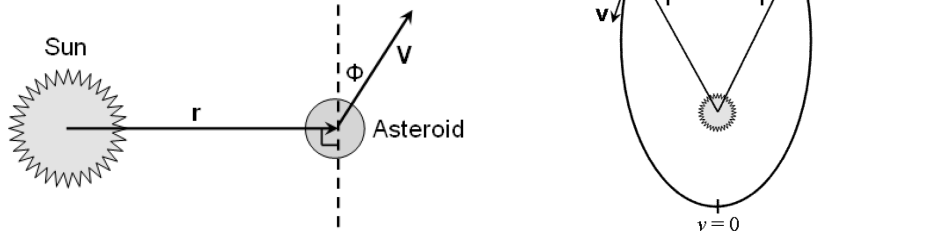

Figure A4

Combining Equations A3.1–A3.3 gives Equation A3.4:

$$\phi = \cos^{-1}\left[\frac{1}{V}\left(\frac{\mu(1+e\cos v)}{r}\right)^{0.5}\right] \tag{A3.4}$$

The specific orbital energy, ε, is given by:

$$\varepsilon = \frac{V^2}{2} - \frac{\mu}{r} \quad \text{or } V = \left(2\varepsilon + \frac{2\mu}{r}\right)^{0.5} \tag{A3.5}$$

Another expression for the parameter, p, using the semi-major axis, a, is given by:

$$p = a(1-e^2) \tag{A3.6}$$

Substituting Equations A3.1, A3.5, and A3.6 into Equation A3.4, and simplifying gives the final expression for ϕ:

$$\phi = \cos^{-1}\left[\frac{(1+e\cos\nu)^2}{2(1+e\cos\nu)-(1-e^2)}\right]^{0.5} \tag{A3.7}$$

Appendix IV: Momentum Balance Relation

The following explains the momentum balance relation:

$$\Delta V = \frac{m_i V_i |\sin\omega_i|}{m_a} + \frac{\Delta P_{ej}}{m_a - \frac{1}{2}m_{ejT}} \tag{A4.1}$$

where ω_i is the angle of impact relative to the asteroid's surface and m_{ejT} is the total mass of all ejecta with initial velocity greater than the asteroid's escape velocity.

Consider a time point right before the impactor hits the asteroid, and a time point after the cratering event. In the reference frame moving at the asteroid's velocity before impact, the momentum balance equation (in the direction tangential to the asteroid's original velocity) is:

$$m_i V_i |\sin\omega_i| = -P_{ej} + \Delta V\left(m_a - m_{ejT}\right) \tag{A4.2}$$

where P_{ej} is the total momentum of the ejecta relative to the reference frame moving at the asteroid's original velocity; however, do not actually calculate that quantity. Instead, integrate the ejecta momentum always relative to the asteroid's instantaneous velocity, to come up with the term ΔP_{ej}. Thus, it is more accurate to derive the momentum balance equation as follows. Consider two changes in velocity, ΔV_1 and ΔV_2. ΔV_1 is caused by the momentum impulse of the impactor itself. Its momentum balance equation in the reference frame of the asteroid before impact is:

$$m_i V_i |\sin\omega_i| = \Delta V_1 \cdot m_a \quad \text{or } \Delta V_1 = \frac{m_i V_i |\sin\omega_i|}{m_a} \tag{A4.3}$$

ΔV_2 comes from the momentum imparted by the ejecta. Its momentum balance equation in the reference frame of the asteroid after ΔV_1 may be approximated by:

$$\Delta V_2 = \frac{\Delta P_{ej}}{m_a - \frac{1}{2} m_{ejT}} \tag{A4.4}$$

Finally:

$$\Delta V = \Delta V_1 + \Delta V_2 = \frac{m_i V_i |\sin \omega_i|}{m_a} + \frac{\Delta P_{ej}}{m_a - \frac{1}{2} m_{ejT}}, \tag{A4.5}$$

which is the equation used in the present simulations. Results from this equation and one in which the $1/2\ m_{ejT}$ term is not included differ by only about 1 part in 10^4.

Appendix V: Relationship of Cratering Constants β and ζ

In cratering equations described in the literature[5,6,7,8,9,10] there are two constants that are commonly presented separately and independently, but for which the present authors have found a simple relationship that holds in the gravity scaling regime.

The constants are most commonly denoted as β and ν. However, denote ν as ζ. The relationship is: $\zeta = \frac{6\beta}{1-\beta}$, or $\beta = \frac{\zeta}{\zeta+6}$, and a derivation of this follows.

The first indication of the relationship came when the following exponent appeared in a derived equation to calculate the required impactor mass to impart a certain momentum impulse via ejecta from a cratering event:

$$\frac{6}{6 - 6\beta + \zeta - \zeta\beta}$$

This exponent would equal 1 if $\beta = \zeta\ /\ (\zeta + 6)$, which seemed more sensible in context than allowing β and ζ to be independent and using various values from the literature, which would cause the exponent to vary slightly around 1 in both directions.

From reference 5:

$$\pi_1 = \frac{Vol \cdot \rho_a}{m_i}, \quad \pi_2 = \frac{g}{V_i^2}\left(\frac{m_i}{\rho_i}\right)^{1/3}, \quad \pi_3 = \frac{Y}{\rho_i V_i^2}, \quad \pi_4 = \frac{\rho_a}{\rho_i} \tag{A5.1}$$

In reference 5, ρ_a is denoted as ρ, ρ_i as δ, V_i as U, Vol as V, and m_i as m.

$$\pi_1 = C\pi_2^{-\alpha}\pi_3^{-\beta}\pi_4^{-\gamma} \tag{A5.2}$$

C and all C_i (see later) are constants.

As noted in reference 5, p. 1852, "It will be assumed that each of ρ and δ are fixed, and any dependence on these variables will not be addressed."

Thus, π_4 is fixed, so one can set $\pi_4^{-\gamma} = C_2$, since γ is a constant. Also, in the gravity regime, π_1 is independent of strength, Y, so we may remove π_3 from Equation A5.2. Now, $\pi_1 = C_2\pi_2^{-\alpha}$.

From reference 6:

$$\pi_D = D\left(\frac{\rho_a}{m_i}\right)^{1/3} \tag{A5.3}$$

Also, because volume, *Vol* is related to diameter, D, by $Vol \propto D^3$,

$$\text{then: } \pi_1^{1/3} = C_3 D\left(\frac{\rho_a}{m_i}\right)^{1/3}, \text{ and } \pi_D = C_4\pi_1^{1/3} = C_4\left(C_2\pi_2^{-\alpha}\right)^{1/3}, \tag{A5.4}$$

$$\text{and : } \pi_D = C_5\pi_2^{-\alpha/3}. \tag{A5.5}$$

(In the derivation of the π groups, described in Part 6, the authors find $\pi_1 = \frac{Vol\cdot\rho_i}{m}$. Because ρ_a/ρ_i is taken here to be constant, this alternate formulation of π_1 can be used in the derivation above of Equation A5.6, with no difference in the results except for the value of C_5.)

From reference 6:

$$\pi_D = C_D\pi_2^{-\beta} \tag{A5.6}$$

Combining Equations A5.6 and A5.7:

$$\beta = \frac{\alpha}{3} \tag{A5.7}$$

From Table 1 in reference 7:

$$\frac{Vol_{ej}(>V)}{R^3} \propto \left(\frac{V}{\sqrt{gR}}\right)^{6\alpha/(\alpha-3)} \tag{A5.8}$$

From reference 6:

$$\frac{Vol_{ej}(>V)}{R^3} = K\left(\frac{V}{\sqrt{gR}}\right)^{\zeta} \tag{A5.9}$$

Combining Equations A5.9 and A5.10:

$$\zeta = \frac{6\alpha}{3-\alpha} \tag{A5.10}$$

Combining Equations A5.8 and A5.11:

$$\zeta = \frac{6\beta}{1-\beta}, \text{ or } \beta = \frac{\zeta}{\zeta+6} \tag{A5.11}$$

Appendix VI: Derivation of π Groups

The crater relations are given by reference 6 as follows:

$$\pi_D = C_D \pi_2^{-\beta}, \text{ where } \pi_D = D\rho_a^{1/3} m_i^{-1/3}, \text{ and } \pi_2 = 3.22gr/V_i^2 \tag{A5.12}$$

This expression for π_2 is consistent with that given in reference 8: $\pi_2 = 1.61gL/V_i^2$, where L is the diameter of the impactor, $L = 2r$. It is also equivalent to the following formulation:

$$\pi_2 = \frac{g}{Q} m_i^{1/3} \rho_i^{1/3}, \tag{A6.1}$$

where Q is the specific kinetic energy (kinetic energy per mass) of the impactor, $Q = 1/2V_i^2$. This assumes a spherical impactor, so that $3.22r = 2m_i^{1/3}\rho_i^{1/3}$. The "mass set" π group is discussed in reference 5, which uses the mass, m_i, the velocity, V_i, and the mass density, ρ_i, to characterize the impactor. The dimensionless quantities are listed as follows:

$$\pi_1 = \frac{Vol \cdot \rho_a}{m_i}, \tag{A6.2}$$

$$\pi_2 = \frac{g}{V_i^2} m_i^{1/3} \rho_i^{1/3}, \tag{A6.3}$$

$$\pi_3 = \frac{Y}{\rho_i V_i^2}, \text{ and} \tag{A6.4}$$

$$\pi_4 = \frac{\rho_a}{\rho_i}, \tag{A6.5}$$

where *Vol* is the volume of the excavated crater, and Y is the strength (units of N/m^2) of the asteroid (or other material being impacted). There is a factor of 2 difference between the formulation for π_2 given by Equation A5.1, and that given by Equation A5.3. The authors use Equation A5.1 in the derivation of the impactor mass vs. ΔV relation, because that is the version used to derive the cratering constants K, C_D, β, and ζ in experiments such as those described in reference 9.

In the present authors' derivation of the "mass set" π group, they get the same quantities as those given in reference 5, with the exception of π_1, which is found to be

$$\pi_1 = \frac{Vol \cdot \rho_i}{m_i}. \tag{A6.6}$$

Besides being a direct result of the mathematics, this formulation is found to be most consistent with the Buckingham Pi Theorem[11] on which the π groups are based, because it allows each π quantity to be independent of the others, that is, any one could be changed without affecting any other. This is not the case for Equations A5.2–A5.4 as written. However, in the discussion of dimensional

analysis using the π groups, reference 5 also says that "It will be assumed that each of ρ_a and ρ_i are fixed, and any dependence on these variables will not be addressed" (p. 1852). Thus π_4 is just a constant, and Equations A5.6 and A5.2 differ only by a constant.

APPENDICES NOTES AND REFERENCES

1. J. A. Burns, "Elementary Derivation of the Perturbation Equations of Celestial Mechanics. *Am. J. Phys.* 44(10) (1976): 944–949.

2. J. A. Burns, "Erratum." *Am. J. Phys.* 45(12) (1977): 1230.

3. R. L. Ward. *The Math Forum* (Drexel University; http://mathforum.org/dr.math/faq/formulas/faq.ellipse.circumference.html).

4. R. R. Bate, D. D. Mueller, and J. E. White. *Fundamentals of Astrodynamics* (Dover Publications, New York, 1971): pp. 16–43.

5. K. A. Holsapple and R. M. Schmidt. "On the Scaling of Crater Dimensions. *J. of Geophysical Research* 87 (B3) (1982): 1849–1870.

6. C. F. Chyba. "Terrestrial Mantle Siderophiles and the Lunar Impact Record." *Icarus* 92 (1991): 217–233.

7. K. R. Housen, R. M. Schmidt, and K. A. Holsapple. "Crater Ejecta Scaling Laws: Fundamental Forms Based on Dimensional Analysis." *J. of Geophysical Research* 88 (B3) (1983): 2485–2499.

8. H. J. Melosh. *Impact Cratering: A Geologic Process* (Oxford Univ. Press, Oxford, 1989): pp. 112–125.

9. R. M. Schmidt and K. R. Housen. "Some Recent Advances in the Scaling of Impact and Explosion Cratering." *Int. J. of Impact Engineering* 5 (1987): 543–560.

10. H. J. Melosh, I. V. Nemchinov, and Y. I. Zetzer. "Non-nuclear Strategies for Deflecting Comets and Asteroids." *Hazards Due to Comets and Asteroids*, T. Gehrels, Ed. (Univ. of Arizona Press, Tucson, 1994): pp. 1111–1132.

11. W. E. Baker, P. S. Westine, and F. T. Dodge. *Similarity Methods in Engineering Dynamics* (Elsevier, 1991): pp. 19–31.